HIGH STRAIN RATE TENSILE TESTING OF ARAMID YARN - A FEASIBILITY STUDY OF OPTICAL MEASUREMENT

Jørgen A. Kepler[1], Lennart E. Hansen[2] and Peter G. Fritsen[3]

[1]Department of Mechanical and Manufacturing Engineering, Aalborg University
Fibigerstræde 16, DK-9220 Aalborg East, Denmark
Email: jk@m-tech.aau.dk

[2]Department of Mechanical and Manufacturing Engineering, Aalborg University
Fibigerstræde 16, DK-9220 Aalborg East, Denmark

[3]Department of Mechanical and Manufacturing Engineering, Aalborg University
Fibigerstræde 16, DK-9220 Aalborg East, Denmark

Keywords: Aramid yarn, Tensile test, High strain rate, Ballistic impact, High speed imaging

ABSTRACT

A method for high-speed tensile testing of dry fiber yarns and registration of strain and force is presented. A combination of established and more recent means, the method combination aims at reducing the registration complexity and synchronicity ambiguity, ideally presenting all necessary data in primary mechanical form, i.e. position, time and mass. The concept is tested and developed using aramid yarns (Kevlar 29) extracted from plain-weave fabric. Due to the discrete temporal and spatial resolution in the high-speed camera images, refinements of lighting condition and tracking software sophistication are recommended for future method development.

1 INTRODUCTION

Aramid fabric is used extensively for absorber backing in composite armor panels, preferably in a dry/semi-dry state (i.e. very low resin saturation), as this facilitates a membrane stress state in the absorber. Ideally, bending stresses are thereby present only in the individual fibers, which, by virtue of the small diameter, approx. 10-15 μm, can accommodate quite small bending radii. Furthermore, aramid fibers may be seen to disintegrate in yet smaller strands (fibrillation, see e.g. the paper by Pauw et al. [5]), which is presumably a principal mechanism behind the resistance of aramid fibers against cutting tools.

In the dry state, a yarn of aramid fibers lends itself poorly to standard mechanical tensile test methods, as it is difficult to provide an even distribution of traction to what is essentially a loose bundle of filaments.

A further complication arises due to the elevated strain rates, often of the order of 10^2 s^{-1} to 10^3 s^{-1} under realistic conditions. Standard test equipment (servohydraulic, lead screw, electromagnetic) is suitable for testing under quasi-static conditions, up to 10^1 s^{-1} (or, with very short specimen gauge length, 10^2 s^{-1}). With suitable modifications to the load application, Zhu et al. [2] demonstrated strain rates in this higher range.

The Kolsky-bar (or Split Hopkinson bar) method may be adapted to tensile testing (e.g. Shim et al. [1]), but the complicated transfer of transient force through the necessary traction grips introduces some ambiguity in the results.

A recent paper by Russell et al. [3] on characterization of UHMWPE describes a testing method which applies the loading in a manner similar to the one outlined in this paper.

Optical strain measurement on aramid yarns at high strain rates was successfully demonstrated by Tapie et al. [4], using high-speed camera, yarn markers and tracking software.

2 EXPERIMENTAL CONCEPT AND SETUP

The present paper outlines a conceptually simple test method, deliberately designed for reduction of measurement ambiguity through application of the most basic mechanical axioms. It must be noted that the method is at present in an initial design stage. However, experiences so far are encouraging. Figure 1 outlines the test setup.

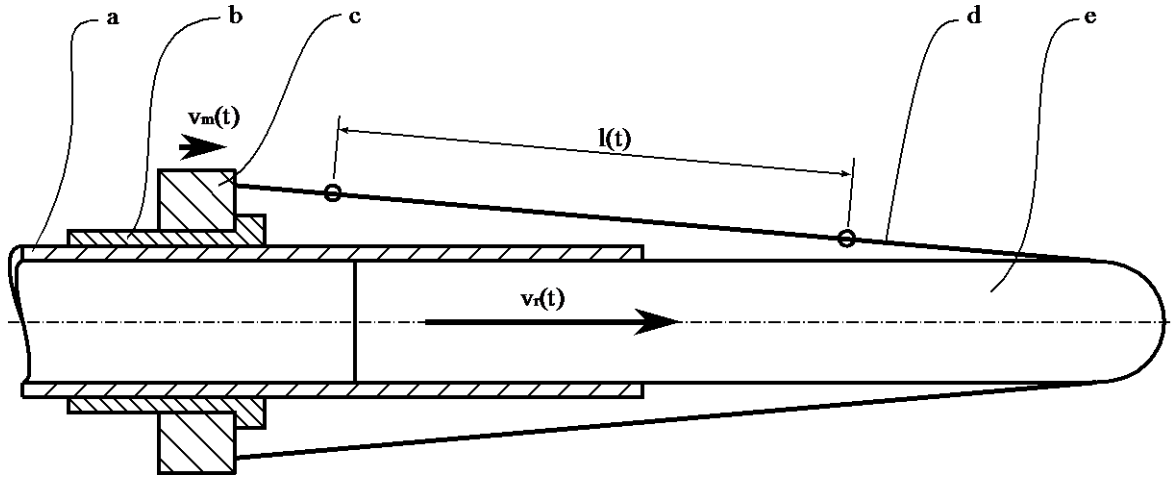

Figure 1: Test setup. a: gas-gun barrel; b: Teflon slider collar; c: Slider mass m; d: yarn; e: rod r

Before testing, the ends of the yarn (d) are fastened to the slider mass (c), which is then placed over the barrel (a) so that the yarn rests over the end of the barrel. A rod (e) with outer diameter 25mm and a rounded front is propelled with a velocity $v_r(t)$ through the barrel, stretching the yarn. The length history l(t) is measured optically, using a high-speed camera (in a fashion similar to [2]) whereby the strain history can be calculated based on the original length l(0) (100 – 150 mm). The applied force is found by deriving the acceleration of mass m from the velocity $v_m(t)$ or by concurrent registration using an accelerometer fixed to the slider mass.

3 DESIGN CONSIDERATIONS – METHOD ADVANTAGES AND DISADVANTAGES

The appeal of this mode of measurement is that, given knowledge of the mass properties, all data necessary derives directly from the time/position data observed through a single camera recording, i.e. a purely kinematic analysis. No principal data are obtained by indirect means (resistive strain gauge data, for example, relies on measuring resistance change and subsequent derivation of strain through amplification and conversion).

While such reduction of processing is desirable, some obstacles may be anticipated: Data for position and time are discrete, as defined by the pixel resolution of the images and the camera frame rate, respectively. The yarn strain can be found directly from the position data, but the slider mass acceleration requires 2 times numerical differentiation of position data.

3.1 Principal considerations for the mechanical test setup

The following assumptions and design considerations are made for the mechanical setup:

1: The masses of rod r and slider mass m are much larger than the yarn mass (the total yarn mass is approximately 0.2 g) to justify the assumption that (2 x) the yarn force equals the slider mass multiplied by the slider mass acceleration

2: The rod and slider masses must be sufficiently high to achieve an approximately constant strain rate in the yarn (their changes in velocity must be small compared to the initial rod velocity v_r).

3: Yarn slip at points of fixation (grips) to the slider mass must be moderate compared to the total yarn length in order to obtain a reasonably constant strain rate

4: The yarn grips and measurement markers should not introduce appreciable stress concentrations

in the yarn

5: The yarn length must be sufficiently short to justify the assumption of uniform yarn strain (the traverse time of a tensile wave must be much shorter than the tensile experiment duration)

In terms of yarn grip design, points 3 and 4 tend to conflict, and the design will be a compromise.

3.2 Yarn grips

Yarn gripping is problematic, due to the multitude of individual fibers, the sensitivity of the yarns to transverse indentation and the relatively low coefficient of friction between yarn and (steel) grip components (the coefficient of friction between a ground steel capstan and aramid yarn was measured to $\mu \approx 0.15$ in a separate experiment). A capstan winding solution was chosen, as this could easily be adopted to both quasi-static and dynamic tests. As is the case with other types of grips, some slip will occur, invalidating strain calculation based on the grip motion. For consolidated composites, or other typical tensile test specimens, strain can be measured using strain gauges, clip gauges or similar, all of which are in direct contact with the specimen. This is not a feasible option for fiber yarns, providing further motivation for optical registration of the selected gauge length strain.

3.3 Yarn markers

Marking the gauge length for optical registration required some experimentation. Initially, two knots were tied at a distance of approximately 100 mm. Experiments demonstrated that knot tightening became significant, changing the effective gauge length. Furthermore, failure invariably occurred at the knots, indicating a significant stress concentration. Secondly, a contrast-color ink was tried; these tend to be rather blurred, as the ink seeps along the fibers. Finally, tying a contrast-color thread around the yarn and fixing it with low-viscosity cyanoacrylate proved effective – the visibility is acceptable, the mass contribution is negligible and it did not introduce appreciable stress concentrations or chemical degradation (yarn failure occurred elsewhere). The three marker methods are illustrated in figure 2.

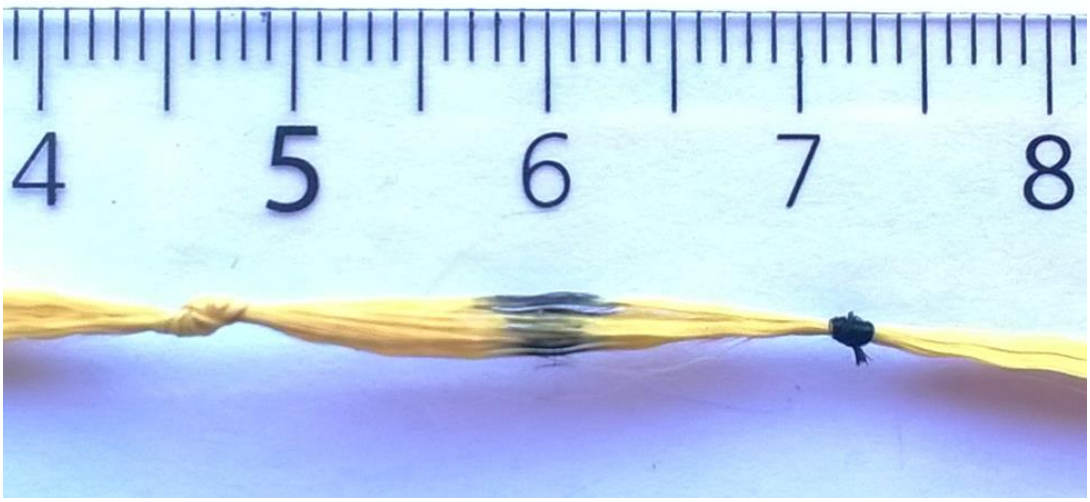

Figure 2: Yarn markers (left to right): Knot, marker ink, thread, against a centimeter scale

3.4 Yarn properties and crimp

The yarns were extracted from plain-weave aramid fabric with a measured weave density of 6.6 yarns/cm, and consequently exhibited some waviness (crimp), see figure 3. The yarn length density was 3300 dtex (3300 gram per 10 km), according to the manufacturer datasheet. Recalculating using an aramid bulk density of 1440 kg/m^3, this corresponds to a yarn (bulk) cross-sectional area of 0.229 mm^2.

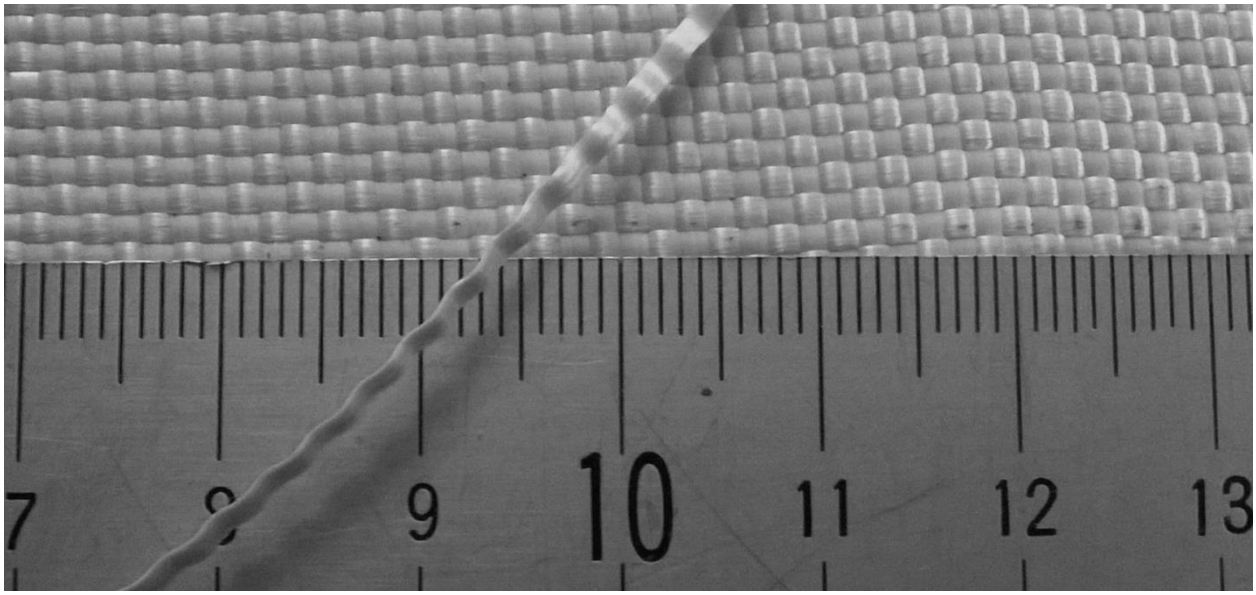

Figure 3: Aramid fabric and extracted yarn, showing yarn crimp, against a centimeter scale.

When subjected to tensile force, the initial deformation of the yarn is associated with straightening, and is therefore not relevant to the material characterization. However, the transition from uncrimping to fiber elongation is gradual. The representative origo of the force/elongation curve may be defined in different manners. As demonstrated below, the present method allows identification of an uncrimping wave, and the temporal origo is defined from the time when that wave reaches the yarn grips.

4 OPTICAL REGISTRATION SETUP, HIGH STRAIN RATE EXPERIMENTS

The experimental setup was located in the Impact Laboratory at Department of Mechanical and Manufacturing Engineering, Aalborg University, where the fixed gas gun and high-speed camera systems could be used with minor modifications to the standard setup. As the gas gun is not designed for operation at such moderate pressures as required in the present test (the gas gun valve is a differential pressure design that relies on sufficient reservoir pressure), an aperture reduction plate was installed for allowing the valve system to work consistently at higher pressure.

The camera is habitually placed inside a protective box made from welded 10mm steel plate, with a small opening for the lens. For further protection, the lens opening is covered by a polycarbonate plate.

Finally, a mirror was used to view the experiment from a more convenient angle.

Figure 4 shows the optical registration setup.

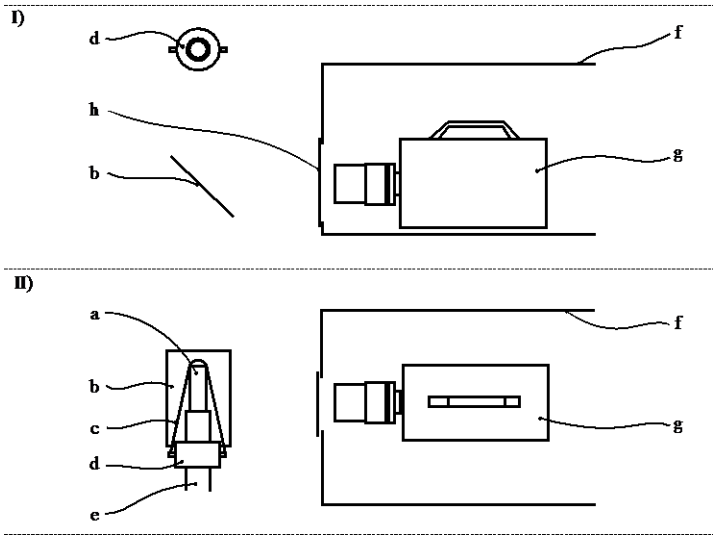

Figure 4: Registration setup seen from the shooting direction (I) and from above (II). The parts are: a: rod, b: mirror, c: yarn, d: slider mass, e: gas gun barrel, f: protection box, g: high-speed camera, h: polycarbonate plate

5 HIGH STRAIN RATE EXPERIMENT – AN EXAMPLE

After performing initial quasi-static tensile tests, a series of experiments were conducted, and strains were derived from optical measurements. As an example, test #3 (of a total of 12 tests) is outlined below. The rod velocity v_r was adjusted iteratively to provide a stable strain rate of approx. 100 s^{-1} while allowing for the extra yarn length outside the gauge sections between the yarn markers.

The experiment was registered using a Photron SA5 high-speed camera, at 30000 frames/second. From test #3, the initial 15 frames (covering 0.5 ms duration) were extracted and examined. Yarn marker locations were registered manually in a bitmap graphics program, i.e. with resolution limited to single pixels.

Figure 5 shows the 3rd frame. The yarn straightening (uncrimping) front is visible about halfway between the yarn markers of both upper and lower yarn.

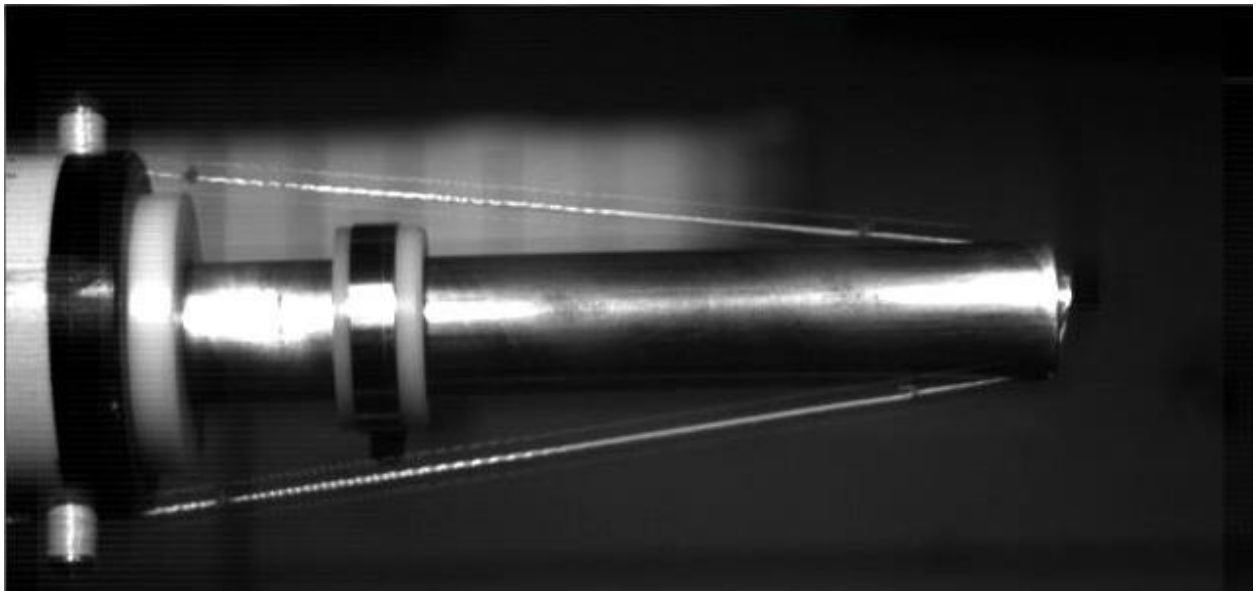

Figure 5: Test #3, 3rd frame, 0.067ms. Yarn uncrimping propagated approx. halfway between yarn markers.

After yarn straightening, the yarn is elongated until failure. Figure 6 shows the frame immediately before failure.

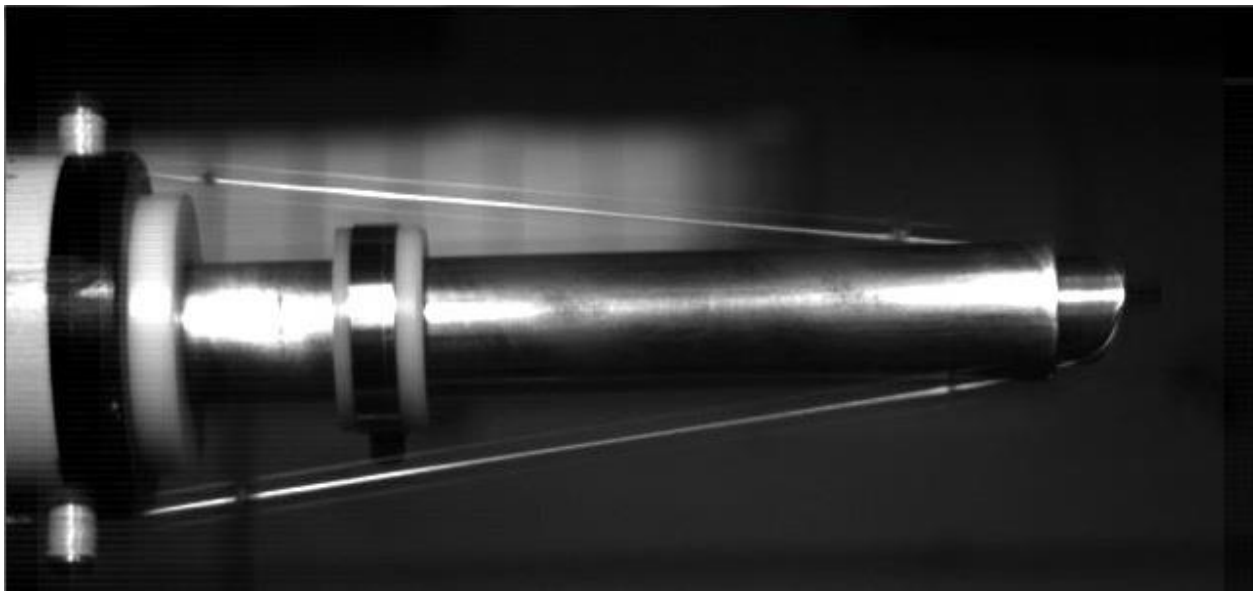

Figure 6: Test #3, 11th frame, 0.333ms. Immediately before yarn failure.

After failure, an unloading wave propagates away from the point of fracture (this point is poorly defined, as the individual fibers fail at different positions. In test #3, failure occurred in the section between the upper and lower yarn, passing over the rod tip, see figure 7.

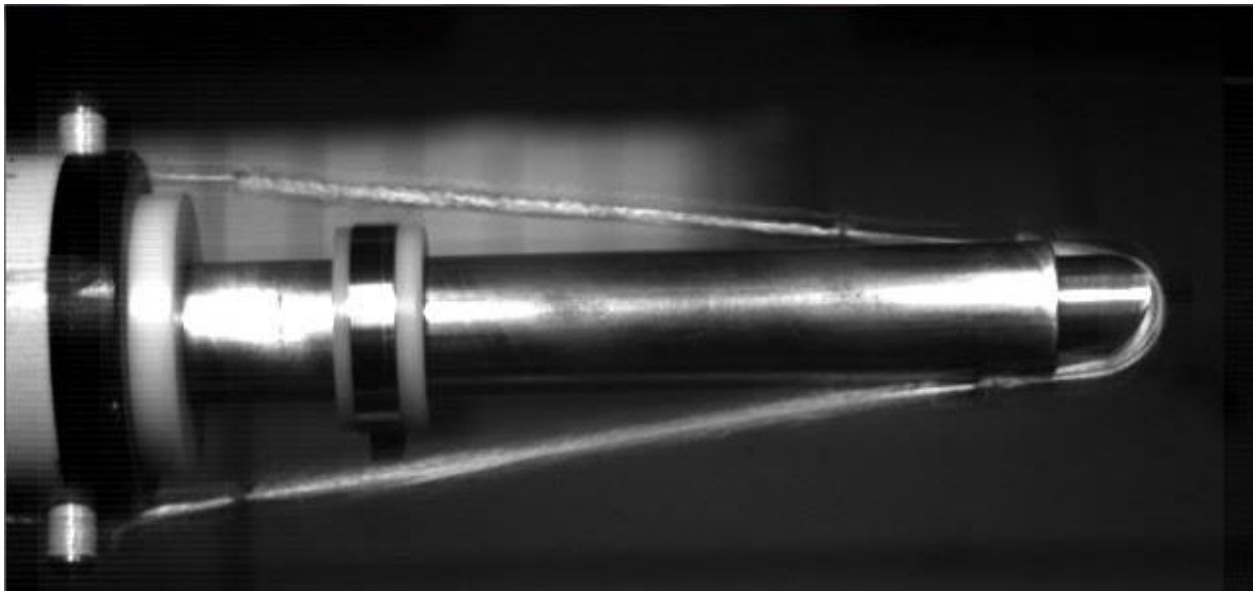

Figure 7: Test #3, 15th frame, 0.467 ms. Failed yarn.

The strain history corresponding to the first 12 frames, as measured between yarn markers on the upper and lower yarn parts, is seen in figure 8.

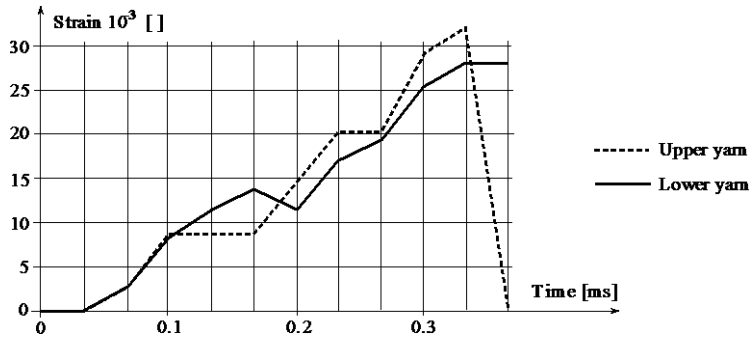

Figure 8: Test #3, strain history.

As seen in figure 8, the failure strain is roughly $30 \cdot 10^{-3}$ and the time of failure $0.33 \cdot 10^{-3}$s, whereby the average strain rate is approximately $30 \cdot 10^{-3} / 0.33 \cdot 10^{-3}\text{s} = 91\text{s}^{-1}$. However, ignoring the uncrimping phase (by starting at the 4th frame, time 0.1 ms), the failure strain is approx. 0.022 and the time of failure $0.23 \cdot 10^{-3}$s, giving a corrected strain rate of 96 s^{-1}. It should be noted that the error sources do not justify a last significant digit error of 1%.

The unevenness of the strain histories could indicate stick-slip at the friction interfaces (rod tip and capstans).

Attempts were made to derive the associated force history from the slider mass motion; however, the motion was typically too small to provide useful slider mass acceleration data (due to 2 times numerical differentiation of the position data). Concurrent measurement data using an accelerometer were extracted. The corresponding force history is shown in figure 9.

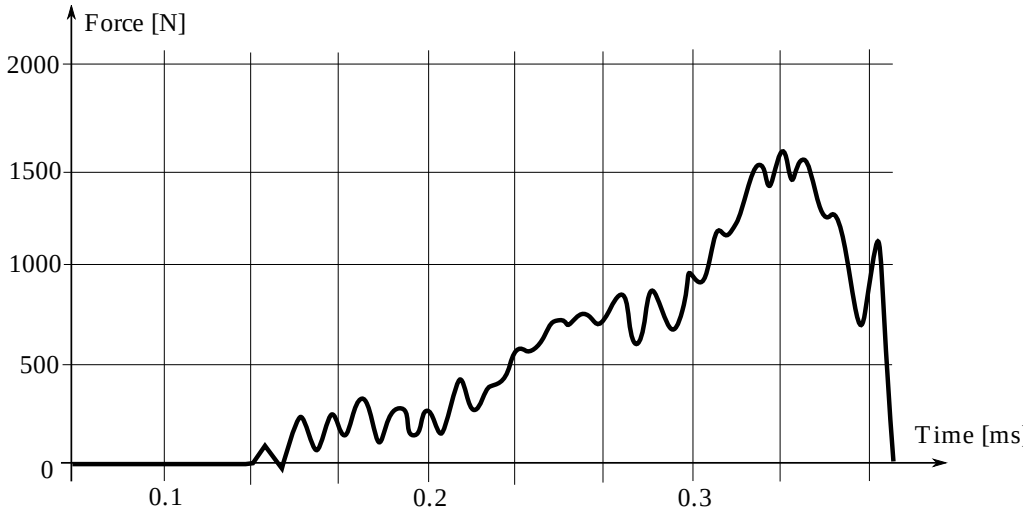

Figure 9: Test #3, force history (slider mass multiplied by acceleration), redrawn from original for clarity

Noting that the force on the slider mass is the sum of forces from upper and lower yarn, the force on one yarn is found by division by 2; similarly, the strain data are averaged between the two yarn halves. The linearized stiffness at this strain rate, when combining force and strain data for corresponding times, becomes approx. $F_{max}/\varepsilon_{fail}$ = 36 kN. An average over 12 tests yielded a stiffness of approx. 40 kN.

6 DISCUSSION AND CONCLUSIONS

By comparison with quasi-static tensile tests, the stiffness at a strain rate of 100 s^{-1} was nearly double.

Some slip between yarns and capstans was observed. This may be reduced by applying a loop yarn method similar to the one described in [3].

The high-speed camera images show “ghost”-contours, presumably caused by the protective polycarbonate shield placed in front of the camera lens and the mirror. As these tests are more controllable than typical ballistic tests, and since the method shows some promise, the setup can be modified to allow omission of shield and mirror.

Position tracking of the slider mass was not feasible with the temporal and spatial resolutions of the equipment. At the time of writing, another approach is being tested, using a rotating mass with a mirror, enabling tracking of a laser beam deflection.

Improvement of the yarn position marker tracking is the single most critical issue. Clearly, a sub-pixel resolution is required. The position marker tracking has relied on manual identification, but image analysis algorithms (similar to edge detection techniques used in commercial Digital Image Correlation) can improve this significantly. Contrast conditions can be refined significantly, reducing tracking marker ambiguity, and allowing better use of the camera’s greyscale range.

Finally, image quality can be improved substantially using pulsed laser illumination, whereby the exposure time can be controlled and synchronized with the camera.

ACKNOWLEDGEMENTS

The work initiated as a student research project, supported by Composhield A/S, manufacturer of composite armor solutions. The support is gratefully acknowledged.

REFERENCES

[1] V. P. W. Shim, C. T. Lim and K. J. Foo, Dynamic mechanical properties of fabric armour, *International Journal of Impact Engineering*, **25**, 2001, pp. 1-15

[2] D. Zhu, B. Mobasher, J. Erni, S.Bansal and S. D. Rajan, Strain rate and gage length effects on tensile behavior of Kevlar 49 single yarn, *Composites: Part A, **43**, 2012, pp. 2021-2029*

[3] B. P. Russell, K. Kandan, V. S. Deshpande and N. A. Fleck, The high strain rate response of Ultra High Molecular-weight Polyethylene: from fibre to laminate, *International Journal of Impact Engineering, **60**, 2013, pp. 1-9*

[4] E. Tapie, V. P. W. Shim and Y. B. Guo, Influence of weaving on the mechanical response of aramid yarns subjected to high-speed loading, *International Journal of Impact Engineering, **80**, 2015, pp. 1-12*

[5] B. R. Pauw, M. E. Vigild, K. Mortensen, J. W. Andreasen, E. A. Klop, D. W. Breiby and O. Bunk, Strain-induced internal fibrillation in looped aramid filaments, *Polymer, **51**, 2010, pp. 4589-4598*